Antimatter from cosmological baryogenesis and the anisotropies and polarization of CMB radiation

Pavel D. Naselsky

Theoretical Astrophysics Center, Juliane Maries Vej 30, 2100 Copenhagen, Ø Denmark,
Niels Bohr Institute, Juliane Maries Vej 30, 2100 Copenhagen, Ø Denmark,
and Rostov State University, Zorge 5, 344090 Rostov-Don, Russia

Lung-Yih Chiang

Theoretical Astrophysics Center, Juliane Maries Vej 30, 2100 Copenhagen, Ø Denmark

We discuss the hypothesis that cosmological baryon asymmetry and entropy were produced in the early Universe by a phase transition of the scalar fields in the framework of the spontaneous baryogenesis scenario. We show that the annihilation of the matter-antimatter clouds during the cosmological hydrogen recombination could distort the CMB anisotropies and polarization by delaying the recombination. After recombination the annihilation of the antibaryonic clouds (ABCs) and baryonic matter can produce peaklike reionization at the high redshifts before quasar and early galaxy formation. We discuss the constraints on the parameters of the spontaneous baryogenesis scenario by the recent WMAP CMB anisotropy and polarization data and on possible manifestation of the antimatter clouds in the upcoming Planck data.

I. INTRODUCTION

The recent release of the first-year Wilkinson Microwave Anisotropy Probe (WMAP) data has confirmed that our Universe is non baryonic dominated. The vast collection of stars, galaxies, and clusters nevertheless contains a huge amount of baryons without strong evidence of antibaryon contamination to the spectrum of electromagnetic radiation in the Universe. Does it mean that starting from the baryogenesis epoch all antibaryons or, more generally speaking, antimatter annihilate with the baryonic matter producing radiation and only a relatively small amount of antibaryons can survive up to the present day during the expansion of the Universe? The answer to this question has been a point of discussion in the literature (see for a review [1–4]) including the big bang nucleosynthesis properties, antiprotons in the vicinity of Earth, and so on. The aim of this paper is to investigate antimatter contamination in the recent cosmic microwave background (CMB) data—namely, WMAP anisotropy and polarization data through distortions of the hydrogen recombination kinetics and possible late reionization of the plasma—and make the corresponding prediction for the future Planck mission.

We reexamine the baryogenesis models following the arguments by [1], in which the baryonic and antibaryonic matter are very nonuniformly distributed at very small scales [for example, the corresponding mass scale can be equivalent to $M \sim (10^3 - 10^5) M_\odot$ [1]] and follow adiabatic perturbation upon these scales. Obviously, the possibility of having a nonuniformly distributed baryonic fraction of matter at very small scales is related to the Affleck-Dine baryogenesis [5] or the spontaneous baryogenesis mechanism [6]. Taking into account the electromagnetic cascades driven by proton-antiproton annihilation at the epoch of hydrogen recombination, we will show how they distort the kinetics of the recombination, producing corresponding features in the CMB

anisotropy and polarization power spectrum. Then we will discuss possible late reionization of hydrogen by the product of annihilation and the corresponding transformation of the CMB anisotropy and polarization power spectrum, taking into account the present WMAP and Cosmic Background Imager (CBI) observational data. Finally we will show that the upcoming Planck mission will be able to detect the corresponding manifestation of matter-antimatter annihilation even if the well-known Sunyaev-Zeldovich y parameter were one order of magnitude smaller than the Cosmic Background Explorer (COBE) Far Infrared Absolute Spectrophotometer (FIRAS) limit [7–9].

II. BARYON-ANTIBARYON BUBBLE FORMATION IN THE UNIVERSE

It is assumed [1] that the scalar baryon of the supersymmetry (SUSY) model ξ is coupled to the scalar inflaton field Φ by the potential

$$V_{int}(\xi, \Phi) = (\lambda \xi^2 + \text{H.c.})(\Phi - \Phi_{\text{crit}})^2, \tag{1}$$

where λ is the coupling constant and Φ_{crit} is some critical value of the Φ field, which determines the point of the minimum of the $V_{int}(\xi, \Phi)$ potential. Starting from the high values $\Phi_{int} \gg \Phi_{\text{crit}}$ the inflaton field decreases down to Φ_{crit} and the $V_{in}(\xi, \Phi)$ potential reaches the point of the minimum, while at $\Phi \ll \Phi_{\text{crit}}$ for the $V_{int}(\xi, \Phi)$ potential we will have $V_{int}(\xi, \Phi) = (\lambda \xi^2 + \text{H.c.}) \Phi_{\text{crit}}^2 = V(\xi)$ independently of the properties of the Φ field. It has been shown [1,2] that because of the properties of the interactions, the most favorable conditions for baryogenesis might be created only for a short time scale. It corresponds to relatively small spatial scales. Thus, the general picture of the baryonic matter-antimatter spatial distribution would be similar to a random distribution of islands with high baryon (or antibaryon) asymmetry float-

ing in normal matter with $\beta = n_{cmb}/n_b \simeq 5 \times 10^{-10}$, where n_{cmb} and n_b are the present number densities of the CMB photons and baryons. The mass distribution function of the baryon (antibaryon) clouds (ABCs) is also estimated [1]:

$$\frac{dn}{dM} \propto \exp\left[-\gamma^2 \ln^2\left(\frac{M}{M_{crit}}\right)\right], \quad (2)$$

where γ and M_{crit} are free parameters of the theory. As one can see from Eq. (2), if $\gamma \gg 1$, then the mass spectrum is localized at $M \sim M_{crit}$, while for $\gamma \sim 1$ the mass spectrum will have monotonic character for the cloud distribution over a wide range of masses. Dolgov and Silk [1] have also pointed out that M_{crit} could be close to the solar mass $M_\odot$, but the range of M_{crit} can be naturally expanded to $(10^3 - 10^5)M_\odot$ [2]. Let us assume that the parameter γ has an especially high value, $\gamma \gg 1$, and the initial distribution function of the baryon-antibaryon clouds is close to the Dirac-δ function, $dn/dM \propto \delta_D(M - M_{crit})$, and the characteristic size of clouds, $R_{cl} \propto M^{1/3}$, is much smaller than the size of the horizon, R_{rec}, at the epoch of recombination ($z \simeq 10^3$): $R_{cl} \ll R_{rec}$. We denote $\rho_{b,in}$ and $\rho_{b,out}$ the antibaryon density inside the clouds and baryon density outside the clouds, respectively, and the mean density $\rho_{b,mean}$ at scales much greater than R_{cl} and distances between them,

$$\rho_{b,mean} = \rho_{abc,in}f + \rho_{b,out}(1-f), \quad (3)$$

where f is the volume fraction of the clouds. We denote

$$\eta = \frac{\rho_{abc,in}}{\rho_{b,out}}. \quad (4)$$

We can write down the following relations between the mean value of the density and inner and outer values:

$$\rho_{b,in} = \frac{\eta \rho_{b,mean}}{1 + f(\eta - 1)} \quad (5)$$

and

$$\rho_{b,out} = \frac{\rho_{b,mean}}{1 + f(\eta - 1)}. \quad (6)$$

Using the functions f and η we can define the antibaryonic mass fraction

$$F_b = \frac{\eta f}{1 + f(\eta - 1)}, \quad (7)$$

which is a function of the characteristic mass scale M_0 of the antibaryonic clouds.

Obviously, all the parameters f, η, and F_b are the results of the fine-tuning of the inflaton $V_{in}(\xi, \Phi)$ leading to the formation of baryonic asymmetry in the Universe.

III. MATTER-ANTIMATTER BARYONIC CLOUDS IN THE HOT PLASMA

At the end of inflation the Universe became radiation dominated by mostly light products of the inflaton decay. Some fraction of matter, however, can exist with a form of primordial antibaryonic clouds. Let us describe the dynamics of such ABC evaporation in the hot plasma. For simplicity we will further assume that a single ABC has a spherically symmetric density distribution $[\rho_{in} \equiv \rho_{in}(r)]$ with the characteristic scale R starting from which the contact between ABCs and the outer baryonic matter leads to an energy release due to annihilation:

$$\frac{dE}{dt} = 4\pi R^2 \varepsilon_{out} v_T = 4\pi R^2 c \varepsilon_{out}\left(\frac{3kT}{2m_p c^2}\right)^{1/2}, \quad (8)$$

where $v_T = (3kT/2m_p c^2)^{1/2}$ is the speed of sound in the plasma, ε_{out} is the energy density of the outer plasma, k is the Boltzmann constant, m_p is the proton mass, and T is the temperature of the outer plasma. Using Eq. (8) and the energy of the inner ABC matter, $E_{cl} = M_{cl}c^2 \sim (4\pi R^3/3)\eta \varepsilon_{out}$, for the characteristic time of evaporation we get

$$\tau_{ev} \simeq \frac{E_{cl}}{dE/dt} = \frac{\eta R}{3c}\left(\frac{3kT}{2m_p c^2}\right)^{-1/2}. \quad (9)$$

Equation (9) indicates that any clouds with size above $R_{cr} \simeq (10^{-5} - 10^{-4})\eta^{-1}(z/z_{rec})^{1/2}r_h(z_{rec})$ will survive up to the moment of the cosmological hydrogen recombination $t_{rec} \simeq 2/3(\Omega_m H_0^2)^{-1/2}z_{rec}^{-3/2}$, where $z_{rec} \sim 10^3$ is the redshift of the recombination, $H_0 = 100h$ is the present value of the Hubble constant, Ω_m is the baryonic plus dark matter density scaled to the critical density, and $r_h(z_{rec})$ is the horizon at the moment of recombination. The baryonic mass at the moment of recombination is of the order of magnitude $10^{19}M_\odot$ [10] and the corresponding mass scale of the ABCs should be roughly $[(10^4 - 10^7)M_\odot]\eta^{-3}$. If the η parameter is close to unity, which means that the density contrast between the inner and outer zones is small, then the corresponding mass scale of the ABCs would be $(10^4 - 10^7)M_\odot$. However, if $\eta \sim 10$, the corresponding mass scale of the ABCs could be smaller and comparable with the scale $(10 - 10^4)M_\odot$.

IV. ABCs AT THE NUCLEOSYNTHESIS EPOCH

Let us compare the characteristic scales of the ABCs with a few characteristic scales of process in the framework of the big bang theory. First, the baryonic fraction of matter and its spatial distribution play a crucial role starting from the epoch when the balance between neutrinos ($\nu_e, \bar{\nu}_e$), neutrons (n), and protons (p) in the reactions $n + \nu_e \leftrightarrow p + e^-$, $n + e^+ \leftrightarrow p + \bar{\nu}_e$, $n \rightarrow p + e^- + \bar{\nu}_e$ is broken. The corresponding time scale of violation of the neutrino-baryon equilibrium is close to $\tau_{\nu_e,p} \simeq 1$ sec when the temperature of the plasma was close to $T_{\nu_e,p} \simeq 10^{10}$ K (see the review in [11]). The time

scale $\tau_{\nu_e,p}$ determines the characteristic length $l_{\nu_e,p} \simeq c\tau_{\nu_e,p}$, which in terms of the baryonic mass fraction of matter corresponds to

$$M_{\nu_e,p} \sim m_{pl} \left(\frac{\tau_{\nu_e,p}}{t_{pl}} \right) \left(\frac{\rho_b}{\rho_\gamma} \right) \bigg|_{t=\tau_{\nu_e,p}} \simeq 0.15 (\Omega_b h^2) M_\odot, \tag{10}$$

where t_{pl} is the Planck time, and ρ_b and ρ_γ are the densities of baryons and radiation in the standard cosmological model without antibaryonic clouds. Following the Standard Big Bang Nucleosynthesis (SBBN) theory we need to specify the moment τ_{end} when all light elements (e.g., He^4 and deuterium) were synthesized during cosmological cooling of the plasma. This moment is of an order of magnitude close to $\tau_{end} \sim 3 \times 10^2 - 10^3$ sec. In term of the baryonic mass scale it corresponds to

$$M_{end} \simeq M_{\nu_e,p} \left(\frac{\tau_{end}}{\tau_{\nu_e,p}} \right)^{3/2} \simeq 5 \times 10^3 \left(\frac{\tau_{end}}{10^3 \text{ sec}} \right)^{3/2} (\Omega_b h^2) M_\odot. \tag{11}$$

Thus, if the characteristic mass scale M_0 for the baryonic clouds is higher than M_{end}, the cosmological nucleosynthesis within each cloud and outside the clouds proceeds independently of others and the mean mass fraction of each chemical element would be the same as in SBBN theory. If all the antibaryonic clouds will annihilate just before or after hydrogen recombination epoch, we will have simple renormalization of the baryonic matter density at the epoch of nucleosynthesis:

$$\rho_{b,out} = \frac{\overline{\rho_b} + \rho_{abc} f}{1-f}, \tag{12}$$

where $\overline{\rho_b}$ is the present day baryonic density rescaled to the SBBN epoch. As one can see from Eq. (12), if the fraction of ABCs is small ($f \ll 1$), then all the deviation of the light-element mass fractions from the SBBN predictions would be negligible.

V. ENERGY RELEASE TO THE COSMIC PLASMA FROM ABCS AT THE EPOCH OF HYDROGEN RECOMBINATION

The net of ABCs produces the net of high-energy photons because of annihilation at the boundary zones for each antimatter cloud. Using Eq. (8), we can estimate the rate of energy injection to the plasma as

$$\frac{d\varepsilon}{dt} = \frac{dE}{dt} n_{cl} = \frac{\rho_{cl} c^2}{\tau_{ev}}, \tag{13}$$

where $\rho_{cl} = M_{cl} n_{cl}$ and n_{cl} is the spatial number density of ABCs. Let us define the mass fraction of ABCs as $f_{abc} = \rho_{cl}/\rho_{out}$ which determines the energy release to the cosmic plasma at the epoch right before and during hydrogen recombination. Because of Compton and bremsstrahlung interac-

tions, the energy density of the products of annihilation leads to the CMB energy spectrum distortion in different ways [12,13]. If τ_{ev} corresponds to the redshift $z>3 \times 10^5 (\Omega_b h^2/0.022)^{-1/2}$, then we should get a Bose-Einstein spectrum

$$n(x,\mu) = [\exp(x+\mu)-1]^{-1}, \tag{14}$$

where $x = h\nu/kT$ (here h is the Planck constant, not the Hubble constant), ν is the frequency of the photons, and μ is the chemical potential:

$$\mu = \mu_0 \exp(-2x_0/x), \tag{15}$$

where $x_0 = 0.018(\Omega h^2/0.125)^{7/8}$. It has been shown [12] that the chemical potential μ is related to the energy release from annihilation by $\mu = 3\rho_{abc} c^2/2\varepsilon_r$, where $\varepsilon_r = 4\pi/c \int I(\nu) d\nu$ and $I(\nu)$ is the intensity of the CMB. For the redshift of annihilation below $z = 3 \times 10^5 (\Omega_b h^2/0.022)^{-1/2}$ the distortions of the CMB power spectrum follows a y-parameter type [14]:

$$n(x) = \frac{1}{\sqrt{4\pi y}} \int d\xi \frac{\exp[-(\ln x + 3y - \xi^2)/4y]}{\exp(\xi) - 1}, \tag{16}$$

where

$$y = \int_0^z \frac{k(T_e - T_{cmb})}{m_e c^2} \sigma_T n_e(z) c \frac{dt}{dz} dz, \tag{17}$$

σ_T is the Thomson cross section, and n_e and T_e are the electron number density and temperature, respectively. The magnitude of the y distortion is related to the total energy transfer by $\kappa = \Delta E/\varepsilon_r = \rho_{abc} c^2/\varepsilon_r = \exp(4y)-1$. At the epoch $10^3 \leq z \leq 10^4$ the COBE FIRAS data give the constraint of the energy release from annihilation $\kappa \leq 2 \times 10^{-4}$, while $y \leq 1.5 \times 10^{-5}$ and $\mu_0 \leq 9 \times 10^{-5}$ at 95% C.L. [7–9].

We would like to point out that the above-mentioned properties of the spectral distortions of the CMB power spectrum are based on the assumption that the distribution of antibaryonic matter is spatially uniform without any clusterization, and therefore, no additional angular anisotropy and polarization of the CMB would have been produced during the epoch of hydrogen recombination. However, the cloudy structure of the spatial distribution of antimatter zones would generate spatial fluctuation of the y parameters, similar to the Sunyaev-Zeldovich effect from hot gas in clusters of galaxies at relatively higher redshift $\sim z_{rec}$. Moreover, such clouds would produce relatively higher but localized y distortions of the CMB power spectrum, which corresponds, in mean, to the COBE FIRAS limit but locally could be much higher.

VI. ELECTROMAGNETIC CASCADES AND HYDROGEN RECOMBINATION

As in the previous section, below we want to estimate the possible influence of the electromagnetic products of annihilation on the ionization balance at the epoch of hydrogen recombination. Using a quantitative approach, we can assume that because of the energy transfer for photons from

$E \sim m_p c^2$ down to $E \sim I = 13.6$ eV, where I is the ionization potential, some fraction $x_e \lesssim 1$ could be reionized by non-equilibrium quanta from electromagnetic cascades in the plasma. The energy balance for such ionization follows

$$I x_e n_{bar} \simeq \omega \varepsilon_r \kappa|_{z \sim z_{rec}}, \tag{18}$$

where ω is the efficiency of the energy transforms down to the ionization potential range and $z_{rec} \simeq 10^3$. From Eq. (18) one obtains

$$\omega \lesssim 5.4 \times 10^{-6} \left(\frac{\Omega_b h^2}{0.022} \right) \left(\frac{1+z}{1000} \right)^{-1} \left(\frac{\kappa}{2 \times 10^{-4}} \right)^{-1} \left(\frac{x_e}{0.1} \right). \tag{19}$$

Thus, the relatively small fraction ($\sim 10^{-5}$) of the annihilation energy release can distort the kinetics of the cosmological hydrogen recombination. The concrete mechanism of the energy transition, starting from $E \simeq m_p c^2 \sim 1$ GeV down to $E \sim I$, is connected to the electromagnetic cascades of the annihilation products with the cosmic plasma. The annihilation of a nucleon and an antinucleon produces ~ 5 pions, 3 of which are charged [15]. For charged pions, an electromagnetic cascade appears due to $\pi^{(+,-)} \to \mu^{(+,-)} + \nu_\mu^{(-,+)}$ decay including the $\mu^{(+,-)} \to e^{(+,-)}$ transition. The neutral pions decay into two photons $\pi^0 \to 2\gamma$. About 50% of the energy release is carried away by the neutrino, about 30% by the photons, and about 17% by electrons and positrons [16]. The spectrum of the decay has a exponential shape $n(E) \propto \exp(-E/E_0)$, where $E \gtrsim E_0 \simeq 70$ MeV [15]. For the electron-positron pair and γ quanta the leading processes of the energy redistribution down to the ionization potential are Compton scattering by the CMB photons and electron-positron pair production $\gamma + (H, He) \to (H, He) + e^+ + e^-$. When $E \gg m_e c^2$, the Compton cross section is well approximated by the Klein-Nishina formula [17]

$$\sigma_C \simeq \frac{3}{8} \sigma_T \left(\frac{m_e c^2}{E} \right) \left[\ln \left(\frac{2E}{m_e c^2} \right) + \frac{1}{2} \right], \tag{20}$$

where σ_T is the Thomson cross section. The corresponding optical depth for the Compton scattering is $\tau_C \simeq 2.1 \sigma_T (m_e c^2 / E_0) \simeq 7.5 \times 10^{-3} \tau_T$, where

$$\sigma_T = 56.7 \left(\frac{\Omega_b h^2}{0.022} \right) \left(\frac{\Omega_m h^2}{0.125} \right)^{-1/2} \left(\frac{1+z}{1000} \right)^{3/2}. \tag{21}$$

For the inverse Compton scattering of high-energy electrons by the CMB photons the corresponding optical depth is $\tau_{IC} \simeq 2 \times 10^9 (\Omega_b h^2/0.022) \tau_C \gg 1$ for $z \simeq 10^3$.

The pair production cross section σ_{pc} has the following asymptotic for $w = E/m_e c^2 > 6$ [18]:

$$\sigma_{He} \simeq 8.8 \alpha_f r_0^2 \ln \left(\frac{513w}{825+w} \right) \tag{22}$$

for neutral helium and

$$\sigma_H \simeq 5.4 \alpha_f r_0^2 \ln \left(\frac{513w}{825+w} \right) \tag{23}$$

for neutral hydrogen, where $r_0^2 = (3/8\pi) \sigma_T$ and α_f is the Fermi constant. Note that for ionized hydrogen and helium which contain 76% and 24% of corresponding mass fractions of the light elements, the optical depth is close to

$$\tau_{pc} \simeq 2.3 \left(\frac{\Omega_b h^2}{0.022} \right) \left(\frac{\Omega_m h^2}{0.125} \right)^{-1/2} \left(\frac{1+z}{1000} \right)^{3/2}, \tag{24}$$

for $wz \gtrsim 825$ [18].

Thus, as one can see from Eqs. (21)–(24), the energy loss for high-energy electrons is determined by the inverse Compton scattering off the CMB photons, whereas for high-energy photons the main process of energy loss is electron-positron pair creation by neutral and ionized atoms.

For the nonrelativistic electrons ($w < 1$) the optical depth inverse Compton scattering is given by $\tau_{IC} \simeq 2 \times 10^9 \tau_T$, whereas for the photons it is close to the Thomson optical depth. It has been shown [17,18] that for high-energy $\to$ low-energy photon conversion the spectral number density is

$$\frac{dn(E)}{dE} \simeq \frac{A}{\sigma_T n_e c} \left(w^{-2} + \frac{14}{5} w^{-1} \right) \tag{25}$$

for $E < E_0$, which corresponds to the energy density

$$\epsilon = \int E dE \frac{dn(E)}{dE} \simeq \frac{14 A m_e c E_0}{5 n_e \sigma_T} \left[1 + \frac{5}{14} \left(\frac{m_e c^2}{E_0} \right) \right]. \tag{26}$$

Therefore, from Eqs. (25), (26) we can estimate the spectral energy density in the range $E \simeq I$:

$$\epsilon(E \simeq I) \simeq \frac{5}{14} \ln 2 \, \epsilon \frac{m_e c^2}{E_0} \simeq 1.7 \times 10^{-3} \epsilon, \tag{27}$$

which is much higher than the limit from Eq. (19). Note that an additional factor of 0.47 results from the fraction of annihilation energy related to the electromagnetic component $\omega \simeq 8 \times 10^{-4}$. As one can see, the nonequilibrium ionization of primordial hydrogen and helium at the epoch of recombination is more effective than the distortions of the CMB blackbody power spectra.

VII. DISTORTION OF THE RECOMBINATION KINETICS

The model of the hydrogen-helium recombination process affected by the annihilation energy release can be described phenomenologically in terms of the injection of additional Ly_α and Ly_c photons [19–21]. For the epochs of antimatter cloud evaporation ($\eta - 1 \ll 1$) the rates of ionized photon production n_α and n_c are defined as
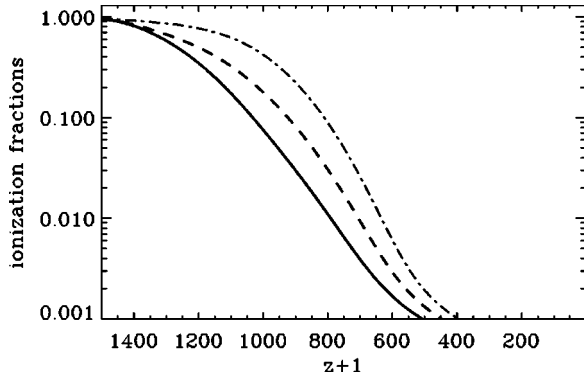
FIG. 1. The ionization fractions for model 1 (solid line), model 2 (dashed line), and model 3 (dash-dotted line) as a function of redshift.

$$\frac{dn_\alpha}{dt} = \varepsilon_\alpha(t)\langle n_b(t)\rangle H(t),$$

$$\frac{dn_i}{dt} = \varepsilon_i(t)\langle n_b(t)\rangle H(t), \tag{28}$$

where $H(t)$ and $\langle n_b(t)\rangle$ are the Hubble parameter and the mean baryonic density, respectively, and $\varepsilon_{\alpha,i}(t)$ are the efficiency of the Ly_α and Ly_c photon production. As one can see from Eq. (28) the dependence of $\varepsilon_{\alpha,i}(t)$ parameters upon t (or redshifts z) allows us to model any kind of ionization regimes. For the ABCs from Eqs. (19), (20) we have

$$\varepsilon_{\alpha,i} \simeq \omega\left(\frac{m_p c^2}{I}\right)[H(t)\tau_{ev}]^{-1} f_{abc}. \tag{29}$$

If the time of evaporation is comparable with the Hubble time $H^{-1}(t)$ at the epoch of recombination $z \sim z_{rec}$, then the $\varepsilon_{\alpha,i}$ parameters are constant and proportional to f_{abc}.

We demonstrate the effectiveness of our phenomenological approach in Fig. 1: the ionization fraction x_e against redshift for the three models

model 1: $\varepsilon_\alpha \simeq \varepsilon_i = 1$;
model 2: $\varepsilon_\alpha \simeq \varepsilon_i = 10$;
model 3: $\varepsilon_\alpha \simeq \varepsilon_i = 100$.

The curves are produced from modification of the RECFAST code [22]. For all models we use the following values of the cosmological parameters: $\Omega_b h^2 = 0.022$, $\Omega_m h^2 = 0.125$, $\Omega_\lambda = 0.7$, $h = 0.7$, $\Omega_m + \Omega_\lambda = 1$, $H(t)\tau_{ev} \sim 1$.

As one can see from Fig. 1 all models 1–3 produce delays of recombination and can distort of the CMB anisotropy and polarization power spectrum, which we will discuss in the following section. We would like to point out that our assumption about the characteristic time of the ABC evaporation—namely, $H(t_{rec})\tau_{ev} \sim 1$—implies that at $t \gg t_{rec}$ all the ABCs disappear. If $H(t_{rec})\tau_{ev} \gg 1$, however, at the epoch of recombination the corresponding influence of the nonequilibrium photons can be characterized by the renormalization of the $\varepsilon_{\alpha,i}$ parameters in the following way: $\varepsilon_{\alpha,i}(z) = \varepsilon_{\alpha,i}(z_{rec})(H(z)\tau_{ev})^{-1}$ where $\varepsilon_{\alpha,i}(z_{rec})$ corresponds to the models 1–3. The mean factor, which should necessarily be taken into account, is the absorption of the high-energy quanta from annihilation by the CMB photons. If, for example, τ_{ev} corresponds to the redshift $z_{rei} \sim 100$, then

$$\varepsilon_{\alpha,i}(z_{rec}) \simeq \varepsilon_{\alpha,i}(z_{rec})\left(\frac{z_{reion}}{z_{rec}}\right)^{3/2} \sim 0.03\varepsilon_{\alpha,i}(z_{rec}). \tag{30}$$

For the relatively early reionization of hydrogen by the products of annihilation, the ionization fraction of matter $x_e = n_e/\langle n_b\rangle$ can be obtained from the balance between the recombination and the ionization processes:

$$\frac{dx_e}{dt} = -\alpha_{rec}(T)\langle n_b\rangle x_e^2 + \varepsilon_i(z)(1-x_e)H(z)\Theta(z_{ev}-z), \tag{31}$$

where $\alpha_{rec}(T) \simeq 4 \times 10^{-13}(T/10^4\ \text{K})^{-0.6}$ is the recombination coefficient, z_{ev} corresponds to τ_{ev}, T is the temperature of the plasma, and $\langle n_b\rangle = n_b$ is the mean value of the baryonic number density of the matter. In an equilibrium between the recombination and the ionization process the ionization fraction of the matter follows the well-known regime

$$\frac{x_e^2(z)}{1-x_e(z)} = \frac{\varepsilon_i(z)H(z)}{\alpha_{rec}(z)n_b(z)}\Theta(z_{ev}-z), \tag{32}$$

where $H(z) = H_0\sqrt{\Omega_m(1+z)^3 + 1 - \Omega_m}$ and $n_b \simeq 2 \times 10^{-7}(\Omega_b h^2/0.02)(1+z)^3$. We would like to point out that Eq. (32) can be used for any models of late reionization, choosing the corresponding dependence of the $\varepsilon_i(z)$ parameter of redshift. This point is vital in our modification of the RECFAST and CMBFAST packages, from which we can use the standard relation for matter temperature $T(z) \simeq 270(1 + z/100)^2 \text{K}$ and all the temperature peculiarities of the reionization and clumping would be related to the $\varepsilon_i(z)$ parameter through the mimicking of ionization history [23,24].

From Eq. (32) one can find the maximal value of the ionization fraction at the moment $z \simeq z_{ev}$:

$$x_e^{max} = -\frac{1}{2}\Gamma + \left(1 + \frac{1}{4}\Gamma^2\right)^{1/2}, \tag{33}$$

where $\Gamma = \varepsilon_i(z_{ev})H(z_{ev})/[\alpha_{rec}(z_{ev})n_b(z_{ev})]$. At $10 \leqslant z < z_{ev}$ the relaxation of the matter temperature to the CMB temperature proceeds faster than the ionized hydrogen becoming neutral and for x_e from Eq. (31) we get

$$x_e(t) \simeq x_e^{max}\left(1 + x_e^{max}\int_{\tau_{ev}}^t \alpha(T)n_b dt\right)^{-1}. \tag{34}$$

While the temperature of matter is close to the CMB temperature T_{CMB}, the corresponding time of recombination is

$$\Delta t_{rec} \simeq \frac{x_e}{|dx_e/dt|} \simeq (x_e^{max})^{-1}t_{rec}(T_{CMB}), \tag{35}$$

where $t_{rec} = [\alpha(T)n_b]^{-1} \ll \tau_{ev}, H^{-1}(t)$.

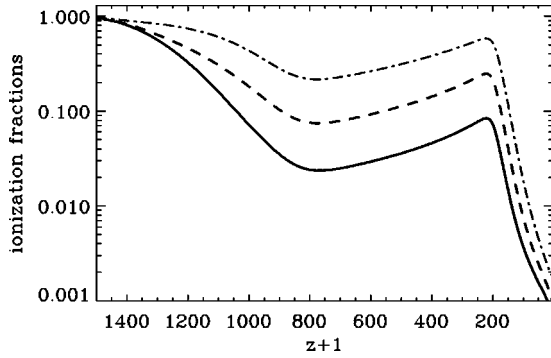In addition to models 1–3 we introduce the three models (see Fig. 2)

FIG. 2. The ionization fractions for model 4 (solid line), model 5 (dashed line), and model 6 (dash-dotted line) as a function of redshift.

model 4: $\varepsilon_\alpha \simeq \varepsilon_i = 0.1 \times [(1+z)/1000]^{3/2}$;
model 5: $\varepsilon_\alpha \simeq \varepsilon_i = 1 \times [(1+z)/1000]^{3/2}$;
model 6: $\varepsilon_\alpha \simeq \varepsilon_i = 10 \times [(1+z)/1000]^{3/2}$,

where $z_{ev} = 200$. In Fig. 3 we plot the ionization fraction for models 4–6 versus redshift. As one can see from Fig. 3 the delay of recombination at $z = 10^3$ is smaller than in Fig. 1, but reionization appears at $z \simeq z_{ev}$. At the range of redshifts, $z \gg z_{ev}$, the behavior of ionization fraction follows Eq. (34) with a rapid decrease. The properties of models 4–6 are similar to those of the peaklike reionization model [24].

VIII. CMB ANISOTROPY AND POLARIZATION FEATURES FROM MATTER-ANTIMATTER ANNIHILATION

In order to find out how sensitive the polarization power spectrum is to the annihilation energy release, we consider phenomenologically different variants of hydrogen reionization models by modifying the CMBFAST code for models 1–6 [25]. One additional problem appears if we are interested in observational constraints on the antimatter fraction abun-
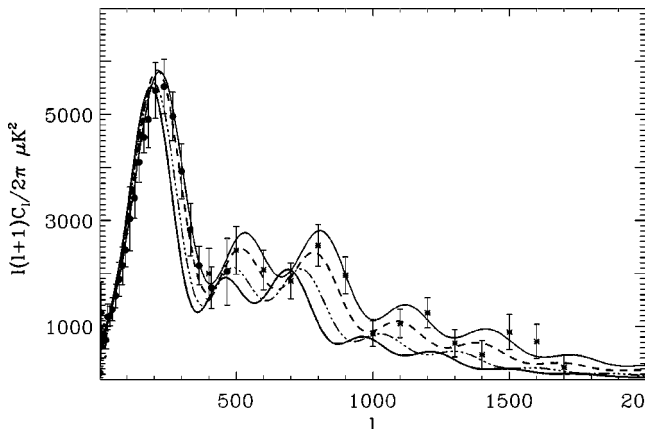

FIG. 3. The CMB power spectrum for the standard model without energy injection (solid line), model 1 (dash line), model 2 (dash-dotted line), and model 3 (the lowest thick solid line) as a function of redshift. For $\ell < 500$ we use the WMAP data [30], while for $\ell > 500$ together with error bars the data is from CBI experiments [31].
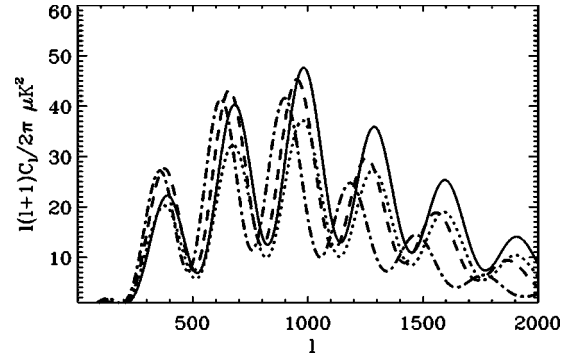

FIG. 4. The polarization power spectrum for the standard model (solid line), model 4 (dotted line), model 2 (dashed line), and model 3 (dash-dotted line) as a function of redshift.

dance related to the late reionization of hydrogen at low redshift $z < 20$. After the WMAP mission the most preferable value of the optical depth of reionization is $\tau_{\text{reion}} \simeq 0.17$ [26], while it is also shown [24] that even the "standard model" with $z_{\text{reion}} = 6$ is not ruled out from the WMAP data (see also [27]). Recently it has been argued that late reionization could exist with two stages, one at $z_{\text{reion}} \simeq 15$ and $z_{\text{reion}} \simeq 6$, due to energy release from different population of stars [28] or heavy neutrinos [29]. Without measurements with a higher accuracy of the CMB polarization and temperature-polarization cross correlation, it is unlikely to settle the issue of late reionization, even for WMAP resolution and sensitivity. However, any assumptions about the optical depth of the late reionization are crucial for an estimation of any constraints on the ABC abundance. If, for example, we adopt the WMAP limit $\tau_{\text{reion}} \simeq 0.17$ from the pure late reionization, the peaklike or delayed recombination models from the ABCs would be restricted very effectively. But if we assume that roughly $\tau_{\text{reion}} \sim 0.04$ comes from late reionization and $\tau_{\text{reion}} \sim 0.06$–$0.12$ is related to ABC contamination at relatively high redshifts, then the constraints on the ABC abundance would be rather smaller than for the previous case. For an estimation of the ABC features in the CMB anisotropy and polarization power spectrum we use a more conservative limit on the optical depth of reionization, $\tau_{\text{reion}} \sim 0.04$ at $z_{\text{reion}} \simeq 6$, in order to obtain the upper limit on the ABC manifestation in the CMB data.

In Fig. 4 we plot the polarization power spectrum $C_p(\ell)$ for models 1–6 plus the standard single reionization model at $z_{\text{reion}} \simeq 6$. The difference between models 1 and 2 mainly lies in the multipoles $2 < \ell < 30$.

As one can see from Fig. 5, in order of magnitude the $\varepsilon_{\alpha,i}$ parameters should be smaller than unity, if $z_{ev} \simeq z_{\text{rec}}$ and $\varepsilon_{\alpha,i} < 10^{-2}$, if $z_{ev} \simeq 200$. So using Eq. (29) one can find that

$$f_{abc} = \omega^{-1} \varepsilon (H(t) \tau_{ev}) \frac{I}{m_p c^2} \lesssim 1.7 \times 10^{-5} \left(\frac{1+z_{ev}}{200} \right)^{3/2},$$

(36)

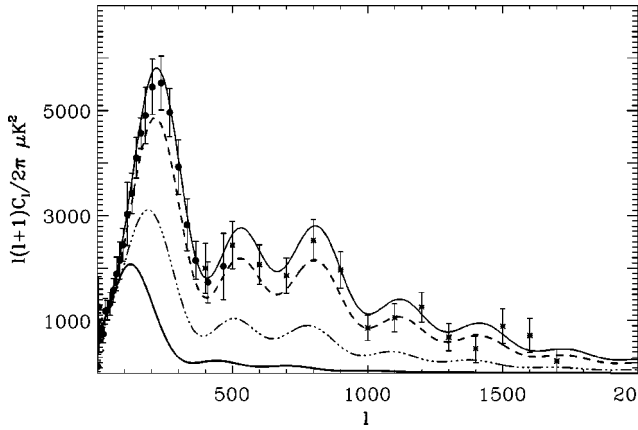while from the spectral distortion of the CMB blackbody power spectra we obtain

FIG. 5. The CMB power spectrum for the standard model without energy injection (solid line), model 4 (dashed line), model 5 (dash-dotted line), and model 6 (lowest thick solid line) as a function of redshift. The experimental data points are the same as in Fig. 3.

$$f_{abc}^{y} \lesssim 1.7 \times 10^{-4} \left(\frac{\Omega_b h^2}{0.022} \right) \left(\frac{1 + z_{ev}}{200} \right). \tag{37}$$

IX. HOW PLANCK DATA CAN CONSTRAIN THE MASS FRACTION OF ANTIMATTER

As is mentioned above, the observational constraint on the antimatter mass fraction f_{abc} depends on the accuracy of the power spectrum estimation from the contemporary and upcoming CMB data sets. As an example of how the upcoming Planck data would be important for cosmology, we would like to compare the upper limit on the f_{abc} parameter, using the WMAP and CBI data with the expected sensitivity of the Planck data. We assume that all the systematic effects and foreground contaminations should be successfully removed and the accuracy of the C_ℓ estimation would be close to the cosmic variance limit at low multipoles for both the temperature anisotropies, polarization, and the TE cross correlation as well (see Fig. 6).

The differences between the delayed recombination and early reionized universe models in comparison with the expected sensitivity of the Planck experiment can be expressed
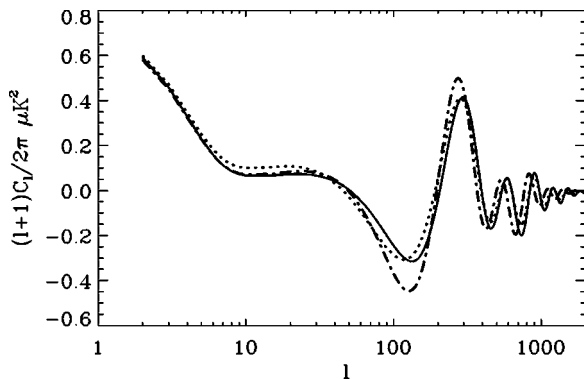

FIG. 6. The TE cross-correlation power spectrum for the models listed in Fig. 4 with the same notation.
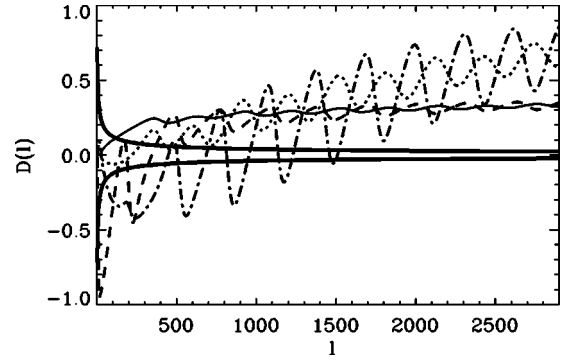

FIG. 7. The $D_{i,j}^{a,p}(\ell)$ function for different models of ionization. The solid line corresponds to $D_{i,j}^{a}(\ell)$ for $i=0$ (standard model without the ABCs) and $j=4$, the dotted line is $D_{i,j}^{a}(\ell)$ for $i=0$ and $j=1$, the dashed line corresponds to $D_{i,j}^{p}(\ell)$ for $i=0$ and $j=4$, and the dash-dotted line is $D_{i,j}^{p}(\ell)$ for $i=0$ and $j=1$. The thick solid lines represent the error bar limit from cosmic variance.

in terms of the power spectrum $C^{a,p}(\ell)$ (for the anisotropy and the E component of polarization) [21]:

$$D_{i,j}^{a,p}(\ell) = \frac{2[C_i^{a,p}(\ell) - C_j^{a,p}(\ell)]}{C_i^{a,p}(\ell) + C_j^{a,p}(\ell)}, \tag{38}$$

where the indices i and j denote the different models and a and p denote anisotropy and polarization. In order to clarify the manifestations of the complex ionization regimes in models 1 and 4 we need to compare the peak to peak amplitudes of the $D_{i,j}^{a,p}(\ell)$ function with the expected error of the anisotropy power spectrum for the Planck experiment. We assume that the systematics and foreground effects are successfully removed. The corresponding error bar should be

$$\frac{\Delta C_\ell}{C_\ell} \simeq \frac{1}{\sqrt{f_{\text{sky}} \left(\ell + \frac{1}{2} \right)}} [1 + w^{-1} C_\ell^{-1} W^{-2} \ell], \tag{39}$$

where $w = (\sigma_p \theta_{\text{FWHM}})^{-2}$, $W_\ell \simeq \exp[-\ell(\ell+1)/2\ell_s^2]$, $f_{\text{sky}} \simeq 0.65$ is the sky coverage during the first year of observations, σ_p is the sensitivity per resolution element $\theta_{\text{FWHM}} \times \theta_{\text{FWHM}}$, and $\ell_s = \sqrt{8 \ln 2} \theta_{\text{FWHM}}^{-1}$.

As one can see from Fig. 7 for $D_{i,j}^{a,p}(\ell)$ the corresponding peak to peak amplitudes are of the order of magnitude of 5–10 times higher than the error bars limit at $\ell \sim 1500$–2500. That means that both anisotropies and the polarization power spectra caused by the complicated ionization regimes can be tested directly for each multipole of the C_ℓ power spectrum by the Planck mission if the systematic effects are removed down to the cosmic variance level. Moreover, at 95% C.L. the corresponding constraint on the f_{abc} parameter can be 2.5–5 times smaller than the limit from Eq. (36), or in principle, the upcoming Planck mission should be able to detect any peculiarities caused by antimatter annihilation during the epoch of hydrogen recombination.

It is worth noting that in this paper we do not discuss the direct contribution of antimatter regions to the CMB anisot-

ropy formation, assuming that their corresponding size is smaller than the typical galactic scales and also smaller than the corresponding angular resolution of the recent CMB experiments such as WMAP, CBI, ACBAR. If the size of the ABCs is comparable with the size of galactic or cluster scales, they could manifest themselves as pointlike sources in the CMB map. For the upcoming Planck mission there are well-defined predictions for the number density of bright point sources for each frequency band in the range 30–900 GHz. It would be interesting to obtain a new constraint on the ABC fraction for large-scale clouds. This work is in progress.

[1] A. Dolgov and J. Silk, Phys. Rev. D **47**, 4244 (1993).

[2] M.Yu. Kholov, S.G. Rubin, and S.G. Sakharov, Phys. Rev. D **62**, 083505 (2000).

[3] J.B. Rehm and K. Jedamzik, Phys. Rev. D **63**, 043509 (2001).

[4] A. Dolgov, in Proceedings of XIVth Rencontres de Blois 2002 on Matter-Antimatter Asymmetry, Blois, France, 2002, edited by J. Tran Thanh Van (unpublished).

[5] I. Affleck and M. Dine, Nucl. Phys. **B249**, 361 (1985).

[6] A. Cohen and D. Kaplan, Phys. Lett. B **199**, 251 (1987).

[7] D.J. Fixen *et al.*, Astrophys. J. **473**, 576 (1996).

[8] J.C. Mather *et al.*, Astrophys. J. **420**, 439 (1994).

[9] M. Bersanelli *et al.*, Astrophys. J. **424**, 517 (1994).

[10] E.W. Kolb and M.S. Turner, *The Early Universe* (Addison-Wesley, Reading, MA, 1994).

[11] K.A. Olive, G. Steigman, and T.P. Walker, Phys. Rep. **333**, 389 (2000).

[12] R.A. Sunyaev and Ya.B. Zeldovich, Astrophys. Space Sci. **7**, 20 (1970).

[13] Y.E. Lybarsky and R.A. Sunyaev, Astron. Astrophys. **123**, 171 (1993).

[14] Ya.B. Zeldovich and R.A. Sunyaev, Astrophys. Space Sci. **4**, 301 (1969).

[15] T. von Egidy, Nature (London) **328**, 773 (1987).

[16] G. Steigman, Annu. Rev. Astron. Astrophys. **14**, 339 (1976).

[17] J. Arons, Astrophys. J. **164**, 457 (1971).

[18] A. Zdziarski and R. Svensson, Astrophys. J. **344**, 551 (1989).

[19] P. Peebles, S. Seager, and H. Hu, Astrophys. J. Lett. **539**, L1 (2000).

[20] A. G. Doroshkevich and P.D. Naselsky, Phys. Rev. D **65**, 123517 (2002).

[21] A. Doroshkevich, I.P. Naselsky, P.D. Naselsky, and I.D. Novikov, Astrophys. J. **586**, 709 (2003).

[22] S. Seager, D.D. Sasselov, and D. Scott, Astrophys. J. Lett. **523**, L1 (1999).

[23] P.D. Naselsky and I.D. Novikov, Mon. Not. R. Astron. Soc. **334**, 137 (2002).

[24] P.D. Naselsky and L.-Y. Chiang, Mon. Not. R. Astron. Soc. **347**, 795 (2004).

[25] U. Seljak and M. Zaldarriaga, Astrophys. J. **469**, 437 (1996).

[26] C.L. Bennett *et al.*, Astrophys. J., Suppl. Ser. **148**, 1 (2003).

[27] B. Ciardi, A. Ferrara, and S.D.M. White, Mon. Not. R. Astron. Soc. **344**, L7 (2003).

[28] R. Cen, Astrophys. J. **591**, 12 (2003).

[29] S.H. Hansen and Z. Haiman, Astrophys. J. **600**, 26 (2004).

[30] G. Hinshaw *et al.*, Astrophys. J., Suppl. Ser. **148**, 63 (2003).

[31] B.S. Mason *et al.*, Astrophys. J. **591**, 540 (2003).